JETIR.ORG ISSN: 2349-5162 | ESTD Year : 2014 | Monthly Issue
JOURNAL OF EMERGING TECHNOLOGIES AND INNOVATIVE RESEARCH (JETIR)
An International Scholarly Open Access, Peer-reviewed, Refereed Journal

Experimental Analysis for the Fundamental Particles

Subhash Chandra and I.D. Joshi

Department of Physics

Faculty of Science

Motherhood University Roorkee,

Haridwar, U.K

`

Abstract

Accelerator field has shown remarkable success and the collision energy in particle colliders has increased exponentially in time which can be described by the \Livingston curve as. At present, about 140 accelerators of all types worldwide are contributing to fundamental research. The present research used high energy data collected by various accelerators mainly at CERN.

INTRODUCTION

This paper primarily deals with the experimental techniques via which high energy data is collected in labs all around the world. As known the development of quantum field theory put the electro-weak and strong forces in one framework and proposes the standard model of particles (M.Gell-Mann, 1964; Quigg, 2009; Sachs, 1955). To validate the standard model we aim to observe phenomena at always higher energy densities and also aim to measure its parameters as precise as possible. To achieve this we need accelerator which are as powerful as possible and detectors which can measure as precise as possible.

During the 20th century particle accelerators have been widely used for physics research and have greatly progressed both scientifically and technologically. Various principles were put forward by scientist all around the world at for example: Van de Graaff "Tendem" accelerator uses the terminal potential difference twice to accelerate the particles (Van de Graaff, Trump, & Buechner, 1947), Betatron work on principle of circular induction and accelerates elections only (Kerst, 1940). In the year 1939 Ernest O. Lawrence was awarded noble for the first modern accelerator, the cyclotron (Sloan & Lawrence, 1931).

Figure 1 *The Livingston curve showing constituent collision energy for different accelerators versus year of completion* (Aßmann, 2002).

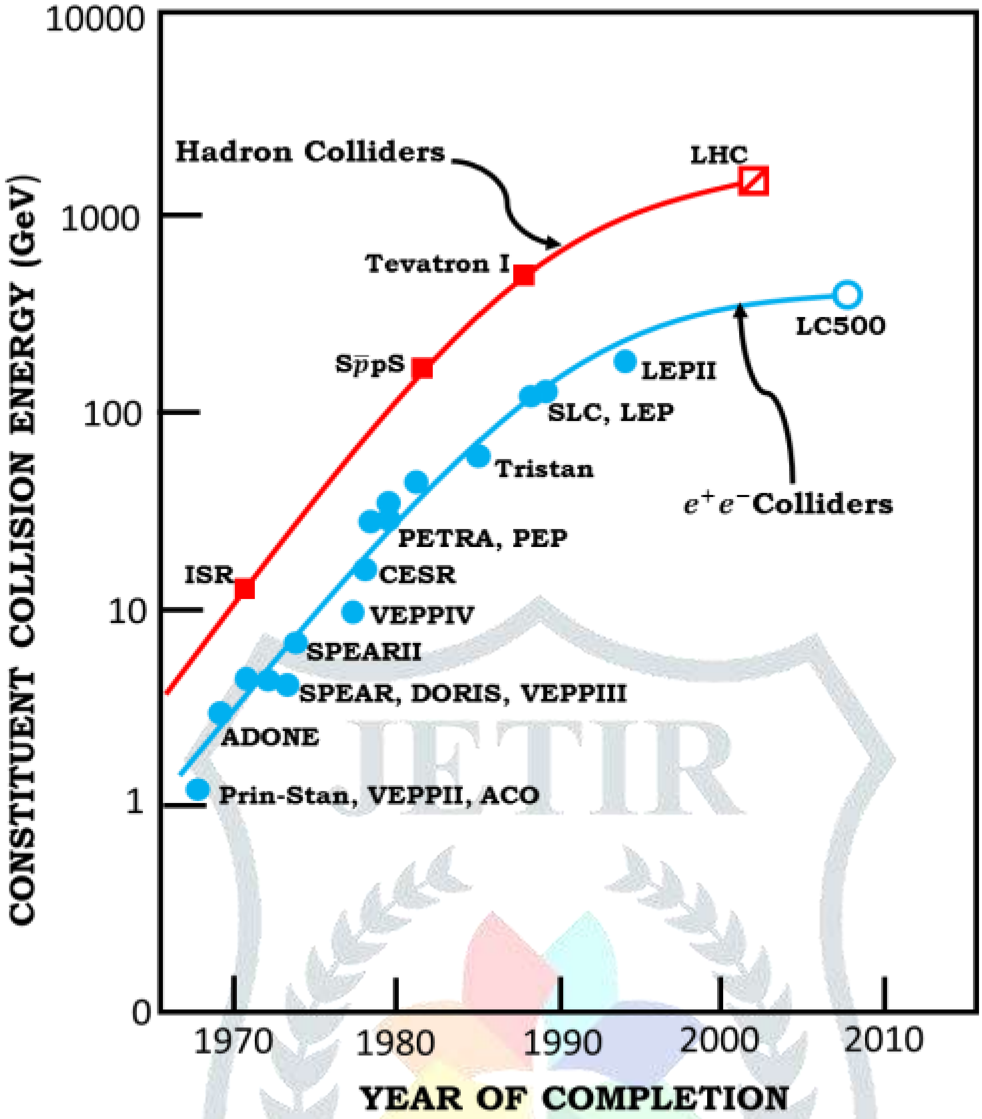

Table 1 *Past and present particle colliders: their particle species, maximum beam energy E_b, circumference or length C, maximum beam luminosity $\mathcal{L}$, and year of luminosity operation (i is for ions; luminosity is in units of $cm^{-1}s^{-1}$).*

AdA	$e+e-$	.25	4.1
VEP-1	$e-e-$	0.16	2.7
CBX	$e-e-$	0.5	11.8
VEPP-2	$e+e-$	0.67	11.5
ACO	$e+e-$	0.54	22
ADONE	$e+e-$	1.5	105
CEA	$e+e-$	3.0	226
ISR	pp	31.4	943
SPEAR	$e+e-$	4.2	234
DORIS	$e+e-$	5.6	289
VEPP-2M	$e+e-$	0.7	18
VEPP-3	$e+e-$	1.55	74
DCI	$e+e-$	1.8	94.6
PETRA	$e+e-$	23.4	2304
CESR	$e+e-$	6	768

PEP	$e+e-$	15	2200
Sp$\bar{p}$S	$p\bar{p}$	455	6911
TRISTAN	$e+e-$	32	3018
Tevatron	$p\bar{p}$	980	6283
SLC	$e+e-$	50	2920
LEP	$e+e-$	104.6	26660
HERA	ep	30+920	6336
PEP-II	$e+e-$	3.1+9	2200
KEKB		3.5+8.0	3016
VEPP-4M	$e+e-$	6	366
BEPC-I/II	$e+e-$	2.3	238
DAΦNE	$e+e-$	0.51	98
RHIC	p, i	255	3834
LHC	p, i	6500	2669
VEPP 2000	$e+e-$	1.0	24
S-KEKB	$e+e-$	7+4	3016

10^{25}	1964
5×10^{27}	1964-68
2×10^{28}	1965-68
4×10^{28}	1966-70
10^{29}	1967-72
6×10^{29}	1969-93
0.8×10^{28}	1971-73
1.4×10^{32}	1971-80
1.2×10^{31}	1972-90
3.3×10^{31}	1973-93
5×10^{30}	1974-2000
2×10^{27}	1974-75
2×10^{30}	1977-84
2.4×10^{31}	1978-86
1.3×10^{33}	1979-2008
6×10^{31}	1980-90
6×10^{30}	1981-90
4×10^{31}	1987-95
4.3×10^{32}	1987-2011
2.5×10^{30}	1989-98
10^{32}	1989-2000
7.5×10^{31}	1992-2007
1.2×10^{34}	1999-2008

THE COLLIDERS

Throughout the first half of the 20th century, the only arrangement for accelerator experiment involved a fixed-target setup, where a beam of charged particles accelerated with a particle accelerator hit a stationary target set into the path of beam. In this setup there was a kinematic disadvantage of producing high center-of-mass energy, as given by equation 2.1 (Perkins & Perkins, 2000).

$$E_{cme} = \left(2E_1E_2 + (m_1^2 + m_2^2)c^4 + 2cos\theta_c\sqrt{E_1^2 - m_1^2c^4}\sqrt{E_2^2 - m_2^2c^4}\right)^{1/2} \quad (2.1)$$

Where c denotes the speed of light. In the above experimental setup this equation becomes, $E_{cme} \approx \sqrt{2E \times mc^2}$ as for high energy accelerators $E \gg mc^2$. For example the collision of $E_b = 7000\ GeV$ proton with a stationary protons $mc^2 \approx 1\ GeV$ can produce reaction with E_{cme} about 120 GeV only. Later more sophisticated experimental setup was employed having kinematic advantage of a high center-of-mass energy resulting in larger momentum transfer called the colliders beam setup in which two beams of particles are accelerated and directed against each other. In this setup the equation 2.1 gives $E_{cme} = 2\sqrt{E_1E_2}$, assuming $\theta_c \approx 0$. In this case two equal mass of colliding particles (e.g., protons and protons, or protons and antiprotons) with same energy of 7000 GeV, one obtains $E_{cme} = 2\sqrt{E_1E_2} = 2E_b = 14000\ GeV$. The idea of exploring collisions in the center of mass system to fully exploit the energy of accelerated particles was first given serious consideration by the Norwegian engineer and inventor Rolf Wideröe (Waloschek, 2013). The figure 2.2 present the most common arrangements of colliding beams. Historically, a single ring was often used for colliding particle and antiparticle beams of equal energy, however modern and future storage-ring colliders (e.g. LHC, BEPC-II, FCC, CEPC, etc.) utilize double ring to achieve extremely high luminosity. The two rings may store particles of the same type, or particles and their antiparticles, or two different particle types, like electrons and hadrons. Hadron collider are 10-20 more energetic then lepton colliders so the path different colliders diverged: hadron colliders continued the quest for record high energies in particle reactions, while in parallel, highly productive $e^{+}e^{-}$ colliders called particle factories focused on precise exploration of rare phenomena at much lower energies.

Figure 2.2 *Illustrates the schematics of particle collider types.*

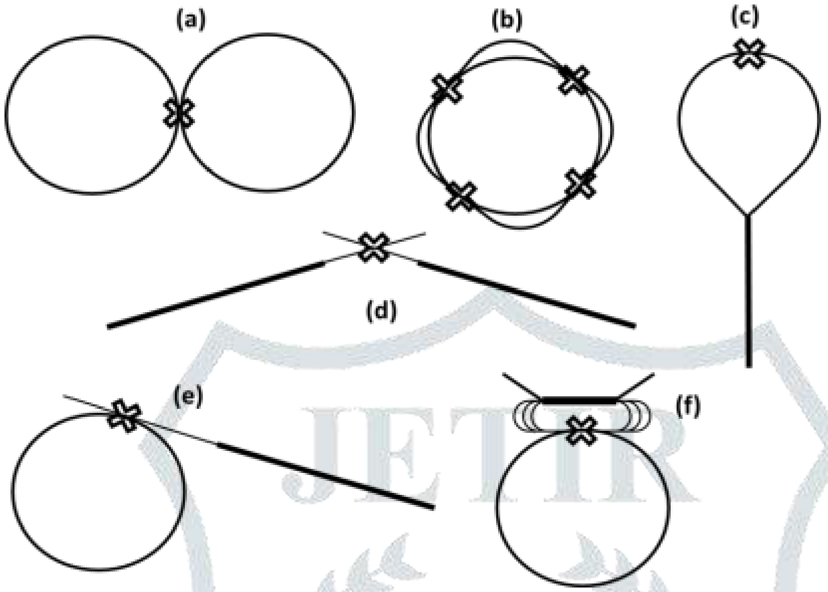

COLLIDER AT CERN

The collider at CERN entitled as Large Hadron Collider (LHC) is a two-ring-superconducting-hadron accelerator and collider installed in the existing 26.7 Km tunnel previously constructed for the Large Electron-Positron collider (LEP). It is designed to provide protonproton collision with unprecedented luminosity ($10^{34}cm^{-2}s^{-1}$) and center-of-mass energy of 14 TeV for the study of rare events such as the production of the Higgs particle. The beams are injected into the LHC form the existing super proton synchrotron (SPS) at an energy of 450 GeV. After the two ring are filled, the machine is ramped to its nominal energy of 7 TeV over about 28 minutes.

Performance Of LHC

At nominal luminosity, the energy stored in each beam is more than 350 MJ. This is more than two orders of magnitude in stored energy, and three orders of magnitude in energy density as shown in the figure
2.3 (a) and (b) (Evans, 2009; Evans & Bryant, 2008).

Figure 2.3 (a) *Energy stored in the accelerator beam, as a function of beam momentum.*

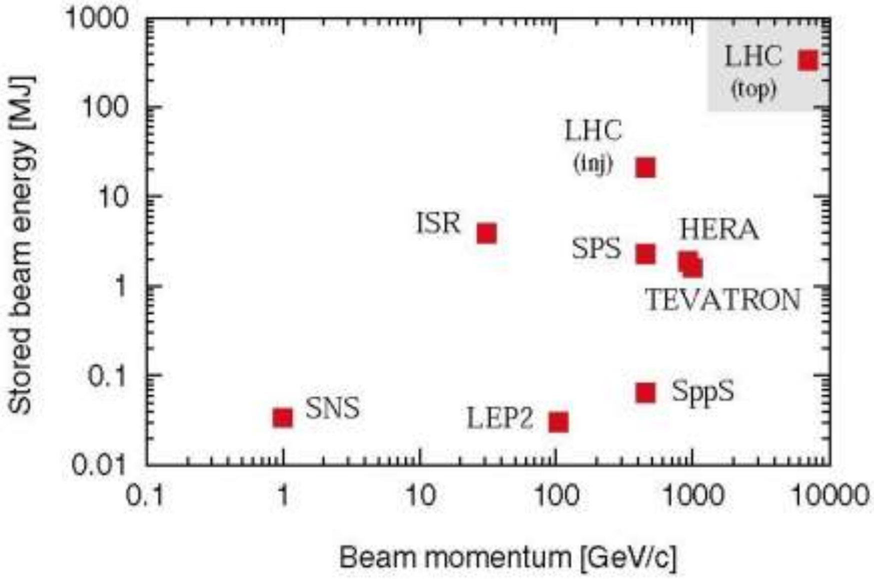

Figure 2.3 (b) *Stored energy density as a function of beam momentum. Transverse energy density is a measure of damage potential and is proportional to luminosity.*

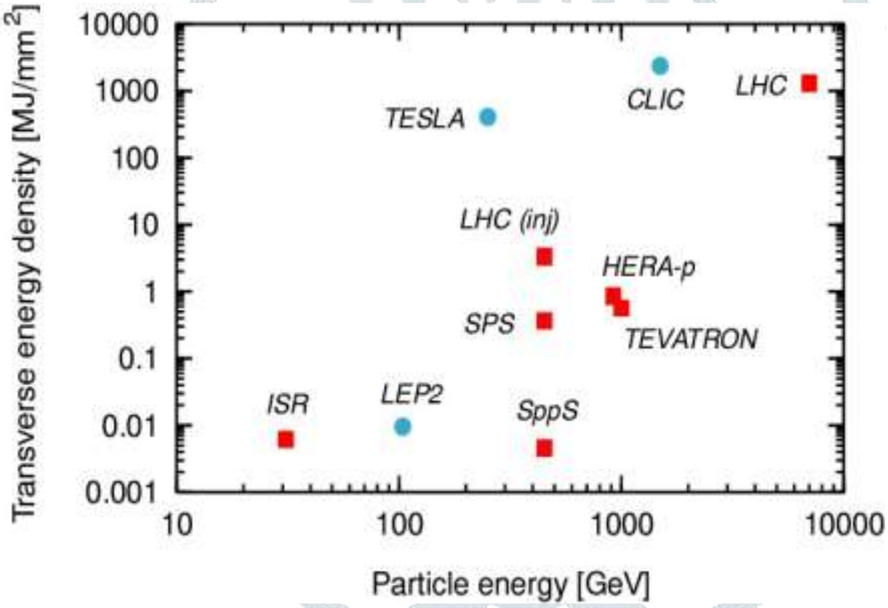

The number of events per second generated in the LHC collision is given by:

$$N_{event} = L\sigma_{event} \quad (2.2)$$

Where σ_{event} gives the cross section for the event under study and L is the machine luminosity. The machine luminosity depends only on the beam parameters and can be written for a Gaussian beam distribution as:

$$L = \frac{N_b^2 n_b f_{rev} \gamma_r}{4\pi \varepsilon_\eta \beta^*} \quad (2.3)$$

Where N_b is the number of particles per bunch, n_b is the number of bunches per beam, f_{rev} the revolution frequency, γ_r the relativistic gamma factor, ε_η the normalized transverse beam emittance, $\beta^*$the beta function at the collision point, and F the geometric luminosity reduction factor due to the crossing angle at the interaction point (IP).

$$F = \left(1 + \left(\frac{\theta_c \sigma_z}{2\sigma^*}\right)^2\right)^{-1/2} \quad (2.4)$$

θ_c is full crossing angle at the IP, σ_z the RMS bunch length, and σ^* the transverse RMS beam size at the IP. Table 2.2 shows the main parameters required to reach a peak luminosity of $10^{34} cm^{-2} s^{-1}$ for proton-proton collisions at 14 TeV center-of-mass. LHC has two high luminosity experiment, ATLAS (Armstrong et al.,

1994) and CMS (Collaboration, n.d.), both aiming peak luminosity of $L = 10^{34} cm^{-2} s^{-1}$ for proton operation, there are two low luminosity experiments: LHCB (Dijkstra, Nakada, Hilke, & Ypsilantis, 1995) and TOTEM (Kienzle et al., 1999).

Table 2.1 *Illustrate performance parameters for LHC*

Parameter	*Value*	*Unit*
Circumference	26.7	Km
Beam energy at collision	7	TeV
Beam energy at injection	0.45	TeV
Dipole field at 7 TeV	8.33	T
Luminosity	10^{34}	$cm^{-2}s^{-1}$
Beam current	0.56	A
Protons per bunches	1.1×10^{11}	
Number of bunches	2808	
Nominal bunch spacing	24.95	ns
Normalized emittance	3.75	μm
Total crossing angle	300	μrad
Energy loss per turn	6.7	keV
Critical synchrotron energy	44.1	eV
Radiated power per beam	3.8	kW
Stored energy per beam	350	MJ
Stored energy in magnets	11	GJ

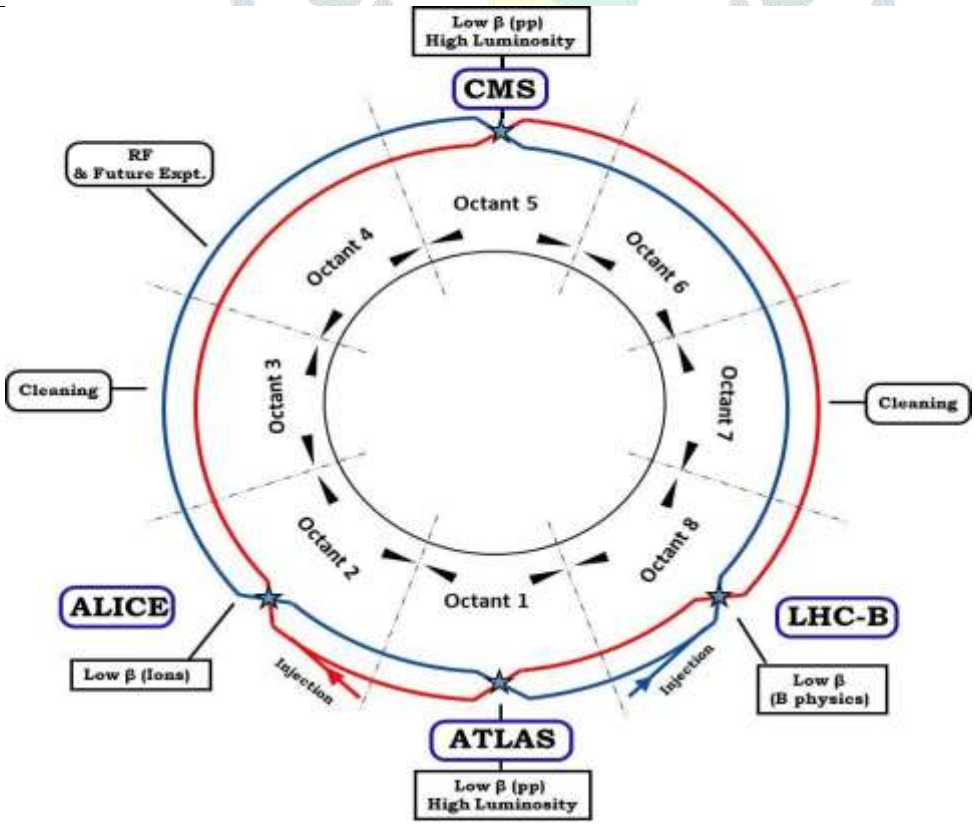

THE CMS DETECTOR

A schematic of Compact Muon Solenoid Experiment (CMS) is shown in figure 2.6. The total weight of the apparatus is 12,500 tons. The detector, which is cylindrical, has a length and diameter of 21.6 m, and 14.6m, respectively. The overall size of the detector is set by the muon tracking system, which in turn makes use of the return flux of a 4 Tesla superconducting solenoid 13m long and 5.9m in diameter.

The core of the magnet coil is also large enough to accommodate the inner tracker and the calorimeter inside. The tracking volume is given by a cylinder 5.8m long and 2.6m in diameter. To deal with high-track multiplicities, CMS employs 10 layers of silicon-microstrip detectors, which provide the required granularity and precision. Additionally there are three layers of silicon pixel detectors to improve the measurement of the impact parameter of charged particle tracks in the position of secondary vertices. The EM calorimeter (ECAL) uses lead tungstate ($PbWO_4$) crystal with coverage in pseudorapidity of up to $|\eta| < 3.0$. The ECAL is surrounded by a brass/scintillator sampling hadron calorimeter with coverage up to $|\eta| < 3.0$ (Buchmüller, 2008). ***Figure 2.6*** *Schematic of CMS detector at LHC.*

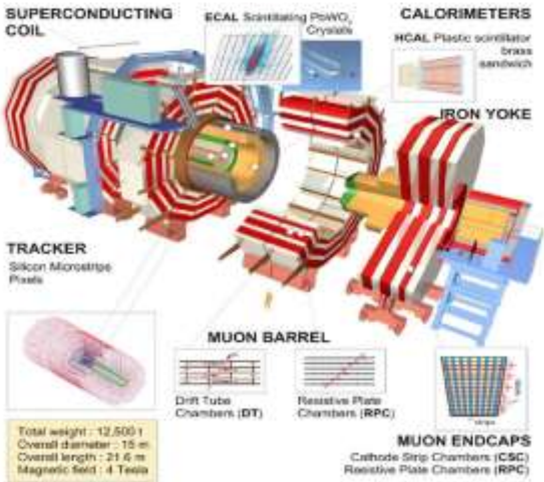

THE ATLAS DETECTOR

ATLAS stands for "a toroidal LHC apparatus". With a length of 46m and diameter of 25m, ATLAS is the largest of all LHC experiments. It is a general purpose detector with: very good calorimetry, including electron and photon identification and measurement, high precision muon momentum measurement; efficient tracking at high luminosities for lepton momentum measurements, electron ID and Photon ID, and heavy-flavor ID; and triggering and measurement a low-pt thresholds. Alhough ATLAS has same performance and physics goals as CMS its design is somewhat different as shown in the figure 2.7 (Buchmüller, 2008).

Figure 2.6 *Schematic of ATLAS detector at LHC.*

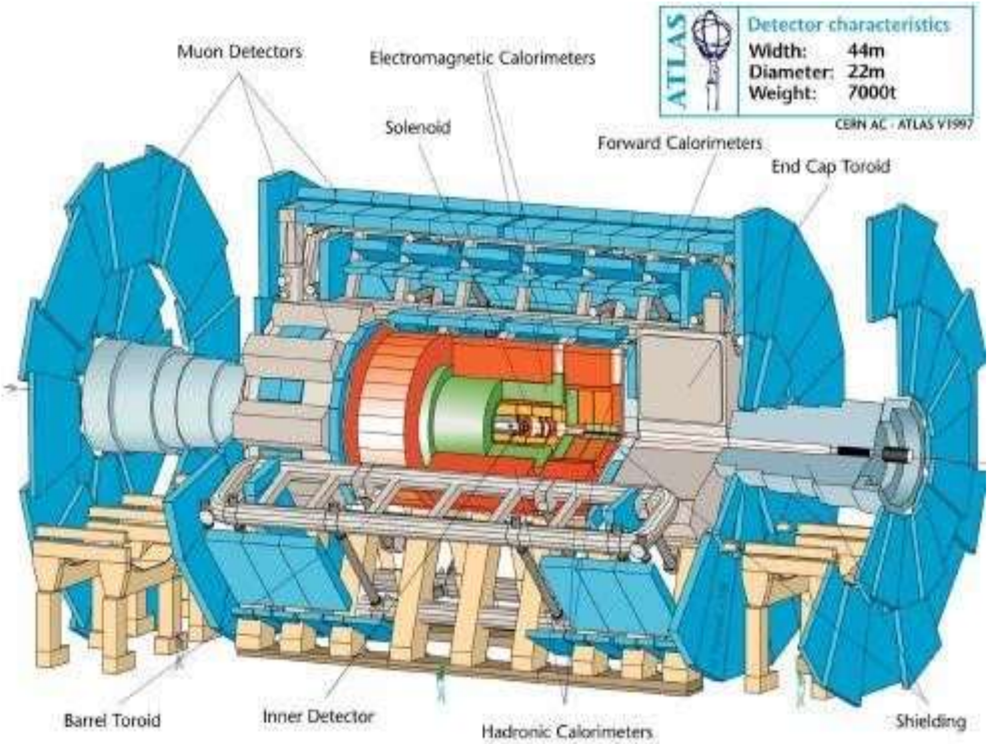

THE LHCb DETECTOR

The LHCb is the experiment for precision measurement of CP violation and rare decays of beauty particles. It consists of the dipole magnet, beam pipe, Vertex Locator, tracking system, and two Ring Imaging Cherenkov detectors (RICH-1 and RICH-2) with three

radiators (Aerogel, C_4F_{10} and CF_4) to achieve excellent $\pi - K$ separation in the momentum range from 2 to 100 GeV/c, a Hybrid photon detectors, the calorimeter system composed of a Scintillator Pad Detectors and Preshower (SPD/PS), an electromagnetic calorimeter (ECAL) and a hadronic (Fe and scintillator tiles) calorimeter (HCAL); the muon detection system composed of MWPC (except in the highest rate region, where triple-GEM's are used). The schematic of the detector is shown in the figure 2.7 (Alves Jr et al., 2008).

Figure 2.6 *Schematic of LHCb detector at LHC.*

References:

Aamodt, K., Quintana, A. A., Achenbach, R., Acounis, S., Adamová, D., Adler, C., … Ahammed, Z. (2008). The ALICE experiment at the CERN LHC. *Journal of Instrumentation*, *3*(08), S08002.

Adriani, O., Bonechi, L., Bongi, M., Castellini, G., D'Alessandro, R., Faus, D. A., … Itow, Y. (2008). The LHCf detector at the CERN large hadron collider. *Journal of Instrumentation*, *3*(08), S08006.

Alves Jr, A. A., Andrade Filho, L. M., Barbosa, A. F., Bediaga, I., Cernicchiaro, G., Guerrer, G., … Marujo, F. (2008). The LHCb detector at the LHC. *Journal of Instrumentation*, *3*(08), S08005.

Anelli, G., Antchev, G., Aspell, P., Avati, V., Bagliesi, M. G., Berardi, V., … Bozzo, M. (2008). The totem experiment at the cern large hadron collider. *Journal of Instrumentation*, *3*(08), S08007.

Armstrong, W. W., Burris, W., Gingrich, D. M., Green, P., Greeniaus, L. G., Hewlett, J. C., … Olsen, W. C. (1994). ATLAS: Technical proposal for a general-purpose pp experiment at the Large Hadron Collider at CERN.

Aßmann, R. (2002). Review of ultra high-gradient acceleration schemes, results of experiments.

Brüning, O., & Rossi, L. (2020). High-luminosity Large Hadron Collider. *CERN Yellow Reports: Monographs*, *10*, 1.

Buchmüller, O. (2008). LHC detectors: commissioning and early physics. In *Journal of Physics: Conference Series* (Vol. 110, p. 12015). IOP Publishing.

Collaboration, A. (n.d.). Technical Design Report, CERN–LHCC 99–14 (May 1999); CMS Collaboration, Technical Proposal, CERN– LHCC 94–38 (December 1994); S. Dawson, D. Dicus, C. Kao, and R. Malhotra.

Dijkstra, H., Nakada, T., Hilke, H. J., & Ypsilantis, T. (1995). *LHCb Letter of Intent, LHCb Collaboration*. CERN-LHCb-95-001.

Evans, L. (2007). The large hadron collider. *New Journal of Physics*, *9*(9), 335.

Evans, L. (2009). The LHC machine. *Proceedings of Science*.

Evans, L., & Bryant, P. (2008). LHC machine. *Journal of Instrumentation*, *3*(08), S08001.

Kerst, D. W. (1940). Acceleration of electrons by magnetic induction. *Physical Review*, *58*(9), 841.

Kienzle, W., Oriunno, M., Perrot, A. L., Weisz, S., Bozzo, M., Buzzo, A., … Buenerd, M. (1999). TOTEM, total cross section, elastic scattering and diffraction dissociation at the LHC: technical proposal.

M.Gell-Mann. (1964). A schematic model of Baryons and Mesons. *Physics Letters*, *8*(3), 214–215. https://doi.org/10.1201/9780429496615

Miucci, A. (2014). The atlas insertable b-layer project. *Journal of Instrumentation*, *9*(02), C02018.

Perkins, D. H., & Perkins, D. H. (2000). *Introduction to high energy physics*. CAMBRIDGE university press.

Quigg, C. (2009). Unanswered questions in the electroweak theory.*Annual Review of Nuclear and Particle Science*, *59*, 505–555. https://doi.org/10.1146/annurev.nucl.010909.083126

Sachs, R. G. (1955). Classification of the fundamental particles. *Physical Review*, *99*(5), 1573–1580. https://doi.org/10.1103/PhysRev.99.1573

Sloan, D. H., & Lawrence, E. O. (1931). The production of heavy high speed ions without the use of high voltages. *Physical Review*, *38*(11), 2021.

Tenchini, R., Aerts, A., van der Stok, P. D. V, Weffers, H., & collaboration, C. M. S. (2008). The CMS experiment at the CERN LHC. *Journal of Instrumentation*, *3*, S08004.

Van de Graaff, R. J., Trump, J. G., & Buechner, W. W. (1947). Electrostatic generators for the acceleration of charged particles. *Reports on Progress in Physics*, *11*(1), 1.

Waloschek, P. (2013). *The infancy of particle accelerators: Life and work of Rolf Wideröe*. Springer Science & Business Media.